

A MAJOR PART
Technical Informa
provide the broad
possible of inform
DOE's Research
Reports to busin
academic commu
state and local go

Although porti
are not reproduc
made available
facilitate the ave
parts of the doc
legible

USE OF THE
n Center is to
it dissemination
on contained in
d Development
s, industry, the
y, and federal,
rnments.

s of this report
e, it is being
microfiche to
bility of those

NOV 05 1987

Los Alamos National Laboratory is operated by the University of California for the United States Department of Energy under contract W-7405-ENG-36

TITLE: A DT FUSION SOURCE BASED ON THE REVERSED-FIELD PINCH

LA-UR--87-3458

DE38 001814

AUTHOR(S): C. G. Bathke, CTR-12
R. A. Krakowski, CTR-12
R. L. Miller, CTR-12
K. A. Werley, CTR-12

SUBMITTED TO: IEEE 12th Symposium on Fusion Engineering

DISCLAIMER

This report was prepared as an account of work sponsored by an agency of the United States Government. Neither the United States Government nor any agency thereof, nor any of their employees, makes any warranty, express or implied, or assumes any legal liability or responsibility for the accuracy, completeness, or usefulness of any information, apparatus, product, or process disclosed, or represents that its use would not infringe privately owned rights. Reference herein to any specific commercial product, process, or service by trade name, trademark, manufacturer, or otherwise does not necessarily constitute or imply its endorsement, recommendation, or favoring by the United States Government or any agency thereof. The views and opinions of authors expressed herein do not necessarily state or reflect those of the United States Government or any agency thereof.

By acceptance of this article, the publisher recognizes that the U.S. Government retains a nonexclusive, royalty-free license to publish or reproduce the published form of this contribution, or to allow others to do so, for U.S. Government purposes.

The Los Alamos National Laboratory requests that the publisher identify this article as work performed under the auspices of the U.S. Department of Energy

A DT FUSION NEUTRON SOURCE BASED ON THE REVERSED-FIELD PINCH

C. G. Bathke, R. A. Krakowski, R. L. Miller, K. A. Werley, Los Alamos National Laboratory, Los Alamos, NM 87545

Abstract. Results are presented from a preliminary scoping study of an ohmically-heated reversed-field pinch (RFP) operating with a steady-state DT fusion neutron wall loading in the range of 1-5 MW/m² while generating less than 100 MW total fusion power. These results are also useful in projecting the development of ignition/burn RFPs, as well as offering an economic source of DT neutrons for fusion nuclear testing.

1. INTRODUCTION

A strong experimental database is evolving from a number of relatively small reversed-field-pinch (RFP) devices.¹⁻⁶ Consequently, the design and construction of the next high-current RFPs are well under way in both the US and the European Economic Community.⁶ More recent studies of the commercial prospects of the RFP as a high-power-density, compact fusion reactor^{7,8} have been completed, showing a strong economic potential should the physics established by existing RFPs extrapolate through the next-step devices to the reactor regime. Preliminary scoping studies of RFPs with characteristics between these next-step devices and the commercial power plant have also been reported.⁹ The characteristics of this spectrum (existing, planned, conceptual) of RFPs are given on Table I.

The main trend in the projections given in Table I is to increase the plasma current and current density, while maintaining the plasma dimensions as small as is allowable by plasma transport, to control the plasma/wall interactions. This trend towards small, high-current plasma reflects the following evolution of the RFP database: (a) nearly constant beta scaling (i.e., $nk_B T \propto I_p^2$); (b) for a fixed value of $I_p/\pi a^2 n$, temperature increases linearly with current (i.e., $T_e \propto I_p$); (c) current densities can be maintained sufficiently high for DT ignition by ohmic heating alone; and (d) plasma confinement at constant beta in ohmically-heated discharge show the confinement time increasing with plasma current ($\tau_E \propto I_p^\nu$, $\nu \approx 0.8-1.5$). These observations along with: (e) robustness of the RFP relaxation or "dynamo" process that maintains stable RFP profiles (i.e., high toroidal field inside the plasma, which decreases to a small value and reverses sign outside the plasma); (f) relatively slow, low-voltage startup and current rampup rates of initially low-energy RFP configurations; and (g) possibility of a variety of current-drive schemes based on low-frequency injection of linked magnetic fluxes (i.e., magnetic helicity injection), has provided the possibility for a relatively direct and inexpensive means to ignite and sustain a burning DT plasma in a compact, high-current-density RFP. This device in its steady-state embodiment would function as a low-to-medium-Q, driven or marginally ignited fusion test facility ("FIF") with a main goal being the generation of fusion-relevant DT neutron currents ($I_n = 1-10 \text{ MW/m}^2$) from plasmas that are sufficiently

small to operate with a total fusion power below ~100 MW and of sufficient $Q (\geq 1)$ to preclude large expenditures in driver power.

Central to the viability and/or feasibility of this compact approach is the ability to manage heat and particle fluxes in a torus that differs little in size from those being planned (Table I). In recognition of this requirement, recent work on the FTF/RFP has emphasized the development of a more detailed understanding of impurity control by magnet divertors.^{10,11} The progress made in modelling edge-plasma processes in the RFP reactor^{9,12} has also added capability to analyzing this problem for the FTF/RFP.

2. APPROACH

The basic approach used in developing a quantitative understanding of the operating space available to an ignition burn RFP, and ultimately to the FTF/RFP, centers around a coupled, time-dependent plasma/first-wall/circuit simulation based on multi-species, profile-averaging, zero-dimension model of the RFP plasma. (Appendix A of Ref. 13, also Ref. 8). A steady-state version of this comprehensive model was used to sweep through a wide range of possible operating points and to identify the main design windows established by present-day technological limits (e.g., stresses, heat fluxes), operation limits (e.g., maximum fusion power, etc.), and limits imposed by the RFP physics database (e.g., transport). Cost estimates were also made, but in the early stages of these analyses only provided guidance. Upon selecting a design point from the steady-state parametric analysis, a two-dimensional vacuum magnetostatics computation was performed to establish the position of the equilibrium-field (EF) and ohmic-heating (OH) coils, subject to the usual constraint imposed by equilibrium and estimated startup (i.e., OHC, stresses, power) requirements. A one-dimensional RFP transport model was used to estimate radial density and temperature profiles, particularly as determined by the impurity seeded, high-radiation plasma needed to smooth heat fluxes in these compact systems. Both the detailed coil configuration and revised plasma profiles were then used in the plasma/circuit simulation to determine the ohmically-heated startup transient leading to oscillating-field current drive¹⁴ and steady state.

3. RESULTS

3.1. Parametric Systems Studies

Parametric results are expressed as contours in a plasma current-radius ($I_p - r_p$) phase space. This phase space is particularly useful in that it measures indirectly two major cost items: (a) coils and power supplies (I_p) and (b) the torus (r_p). Table II lists all parameters that were held fixed during this phase of the study, with a simplified (analytic) coil model⁹ indicating $A \geq 6$ in order to keep comparable the ohmic power requirement in the PFC and plasma

TABLE I. MAIN PARAMETERS FOR EXISTING (E), PLANNED (P), AND CONCEPTUAL (C) RFP DEVICES

Device	Status	Laboratory	Ref.	Major Radius R_T (m)	Minor Radius r_p (m)	Plasma Current I_p (MA)	Plasma Current Density j_p (MA/m ²)	Electron Temp. T_e (keV)	Average Density n (10 ²⁰ /m ³)	Pooidal beta β_p
TPE-IR(M)	E	ETL/Japan	1	0.10	0.09	0.13	5.1	0.60	0.3	0.1
ETA-BETA II	E	Pedova/Italy	2	0.65	0.125	0.15	3.0	0.60	1.0	0.1
HBTX-1A	E	Culham/UK	3	0.60	0.18	0.32	1.5	0.10	0.2	0.05
OHTE/RFP	E	GA/USA	4	1.14	0.20	0.50	4.5	0.4-0.6	0.5-3.0	0.1-0.2
ZT-40M	E	LANL/USA	5	1.14	0.20	0.44	3.5	0.3-0.5	0.4-0.9	0.1-0.2
RFX	P	Pedova/Italy	6	2.00	0.48	2.0	2.8	0.5-2.0	0.3-2.0	0.10
ZTH	P	LANL/USA	6	2.40	0.40	4.0	6.0	0.5-5.0	0.3-5.0	0.10
FTF/RFP	C	LANL Study	9	1.80	0.30	10.4	37	10-20	6.0-9.0	0.1-0.20
TITAN	C	UCLA-led Study	8	3.60	0.6	18.2	14	10-20	2-3	0.1

TABLE II. FIXED BASECASE PARAMETERS FOR FTF/RFP

Effect plasma atomic number, Z_{eff}	1
Anomalous ohmic heating of ions, f_{OHAI} ^(a)	0
Plasma aspect ratio, $A = R_T/r_p$	6.
Transport scaling parameter, $\nu(\tau_{ce} \propto I_p^2 r_p^2)$	1.25
Poloidal beta, β_p	0.10
Fraction of alpha-particle energy to plasma, f_α	1.0
Pinch Parameter, $\Theta = B_\theta(r_p)/(B_\phi)$	1.45
Reversal Parameter, $F = B_\phi(r_p)/(B_\theta)$	-0.11
Density and temperature profiles	cubic ^(b)

(a) Actually observed in RFP experiments.

(b) Subsequently modified by one-dimensional results when the time-dependent plasma/circuit simulation was made.

The parametrics model generates on a plot of I_p versus r_p lines of constant neutron wall loading, I_w (MW/m²), average first-wall heat flux, q_w (MW/m²), total fusion power, P_F (MW), constant electron or ion temperature, $T_{e,i}$ (keV), constant electron density, n_e (m⁻³), constant electron streaming parameter, $\xi = v_D/v_{th,e}$, constant current density, j_ϕ (MA/m²), constant plasma loop voltage, V_ϕ (V), constant Lawson parameter, $n\tau_E$ (s·m²), and constant ignition parameter, $f_\alpha P_\alpha / [f_\alpha P_\alpha + P_{\Omega p} (1 + f_{OHAI})]$, where P_α is the alpha-particle power, $P_{\Omega p}$ is the plasma ohmic dissipation, and f_{OHAI} accounts for possible anomalous heating of the ions, as is observed experimentally. Selecting the following range for key variables defines the design window used to guide this study: $I_w = 1$ -5 MW/m², $P_F < 100$ MW, and $q_w < 5$ MW/m².

The design window resulting from this analysis is shown on Fig. 1 for the basecase parameters listed in Table II. Table III lists the main parameters for an $r_p = 0.3$ -m device operated at either $I_w = 1$ MW/m² or 5 MW/m²; the former case is highly driven ($Q_p \equiv P_F/P_{\Omega p} = 0.8$), whereas the latter is marginally "ignited"

TABLE III. DEVICE PARAMETERS FOR FTF/RFP

Parameter	Fusion Neutron First-Wall Loading	
	1 MW/m ²	5 MW/m ²
Plasma major radius, R_T (m)	1.8	
Plasma minor radius, r_p (m)	0.3	
Plasma shape	circular	
Plasma volume, V_p (m ³)	3.20	
First wall area, A_{FW} (m ²)	23.25	
Blanket/shield thickness, Δb (m) ^(a)	0.30	
Blanket/shield volume, V_{BSL} (m ³)	10.23	
Poloidal field at plasma edge, B_θ (T)	5.62	6.96
Toroidal field at plasma edge, B_ϕ (T)	-0.43	-0.53
Safety factor, $q(r_p) \approx F /\Theta A$	~0.015	
Average electron temperature, T_e (keV)	4.33	9.29
Average ion temperature, T_i (keV)	4.20	8.95
Average electron density, n_e (10 ²⁰ /m ³)	9.22	6.60
Toroidal plasma current, I_ϕ (MA)	8.44	10.44
Plasma current density, j_ϕ (MA/m ²)	29.8	36.9
Lawson parameter, $n\tau_E$ (10 ²⁰ s/m ²)	1.44	1.40
Ohmic power in plasma, $P_{\Omega p}$ (MW)	33.2	17.1
Fusion power, P_F (MW)	26.7	133.
Plasma Q-value, $Q_p = P_F/P_{\Omega p}$	0.80	7.78
First-wall heat flux, q_w (MW/m ²)	1.81	2.96
Plasma loop voltage, V_ϕ (V)	3.94	1.64
Streaming parameter, $\xi = v_D/v_{th,e}$	0.0052	0.0061

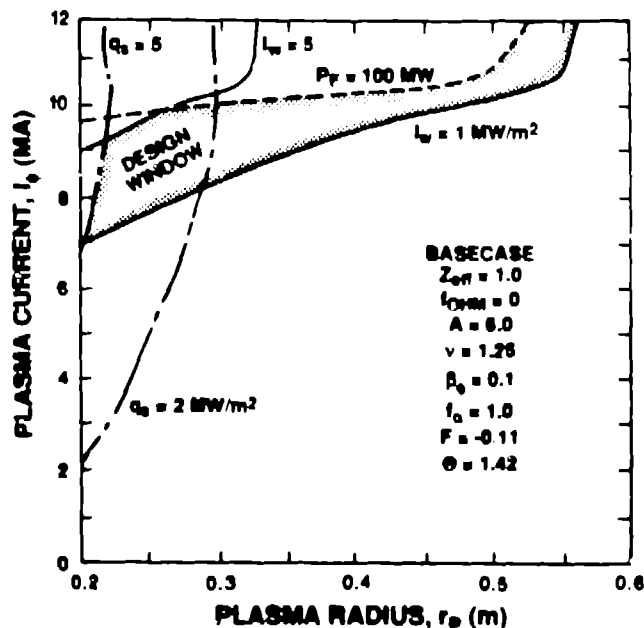


Fig. 1. Ohmically-heated FTF/RFP design window formed by total-power, neutron wall loading, and average-heat-flux constraints for the fixed parameters given in Table I.

($Q_p = 8.8$). The sensitivity of the design window constructed in Fig. 1 to changes in the main physics parameters, β_p , ν , and f_{OHAI} is demonstrated in Fig. 2.

3.2. Magnetics Configuration

The design-point determination described in the previous section was guided by an approximate magnetics model based on a bipolar OHC swing and a desire to minimize ohmic losses at steady state.⁹ A two-dimensional vacuum magnetics code, CCOIL, was used to establish the details of a closely coupled OHC and EFC set subject to the usual equilibrium, stress, and power constraints, with the latter two being estimated from a plasma circuit time-dependent simulation (Sec. 3.3) using the results of Table III, profile modifications for a highly radiating plasma, and the CCOIL calculations.

The OHC/EFC set was nominally positioned a distance from the plasma, Δb , equal to the plasma radius, $r_p \approx 0.3$ m. Both OHCs and EFCs were taken to be fabricated from copper alloy, since for the sizes being considered the power consumption could be held to acceptable limits. Likewise, a close-fitting, efficiently coupled geometry was chosen under the assumption that if the size could be minimized a single-piece "clam-shell" configuration could be adopted to gain access to the inner torus for maintenance purposes. The position of the EFCs satisfied both the equilibrium vertical-field constraint and a field-decay index in the range $0 < (-\partial(nB_z)/\partial(nr)) \leq 0.65$. Coil positions are optimized so that magnetic flux from the back-biased OHC is excluded from the plasma chamber to a level that met maximum vertical-field constraints for efficient plasma breakdown; because of the low toroidal fields in the RFP, this constraint is more serious than for the tokamak.

Figure 3 gives a cross-sectional view of the closely coupled OHC/EFC geometry that results from the CCOIL computation for the $I_w = 5$ -MW/m² design. This coil set is illustrated in the back-biased condition, with a strong octapole null indicating good promise for breakdown. The main OHC and EFC parameters are

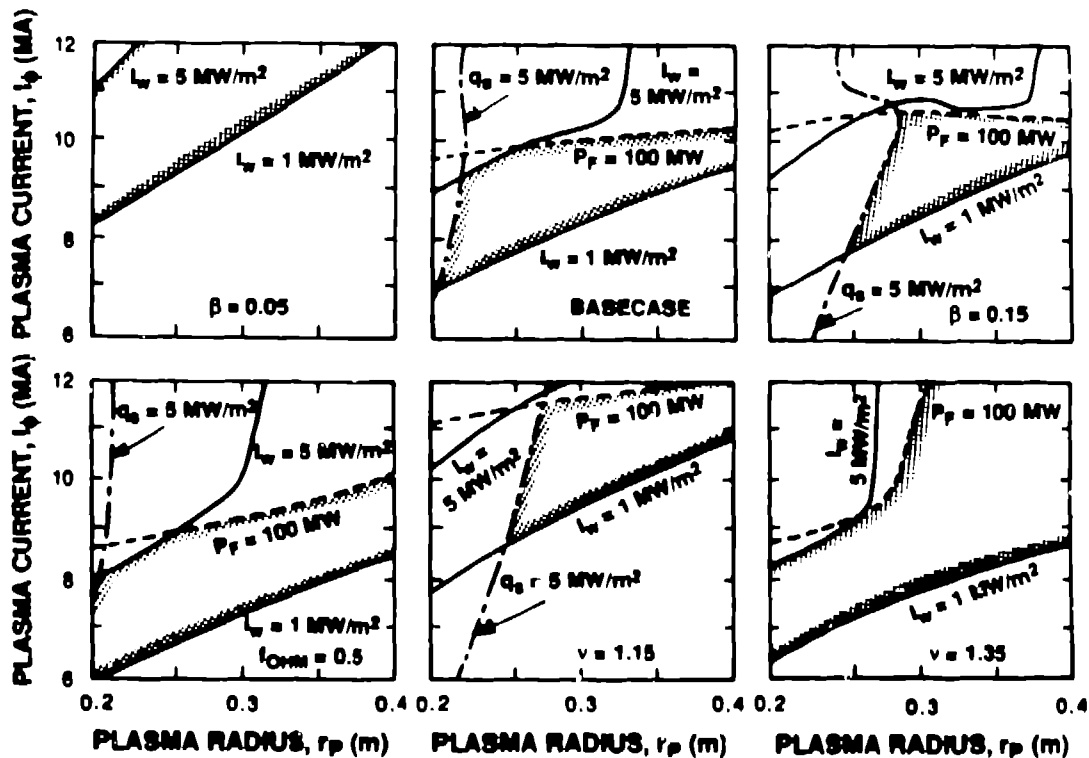


Fig. 2. Sensitivity of FTF/RFP design window to departure from the Table I basecase values for β_0 , ν , and f_{OHM} .

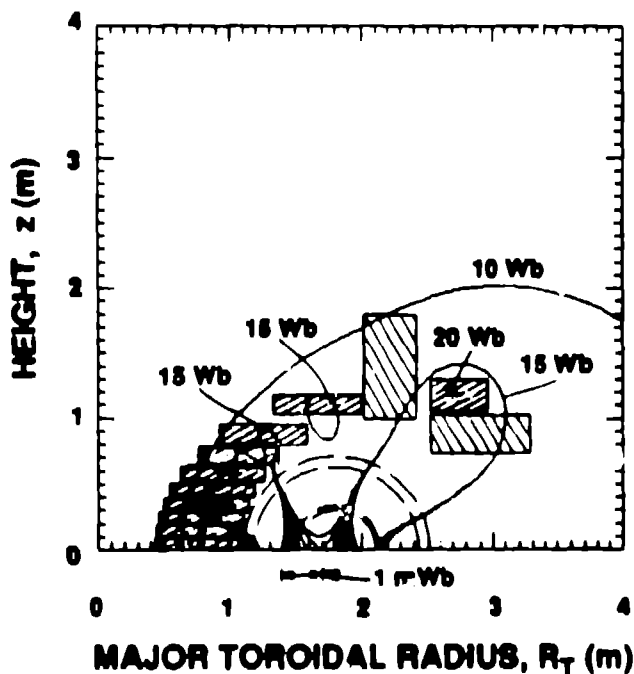


Fig. 3. Closely coupled OHC and EFC coil set for FTF/RFP showing the flux plot and field null in the back-biased condition.

3.3. Startup Simulation

The one-dimensional profiles, coil parameters, and general guidance provided by the steady-state parametrics study were combined into the time-dependent plasma/circuit simulation model. Initial conditions were derived from a separate RFP breakdown/formation model developed from experimental data.⁹ Typical plasma and circuit responses are shown in Fig. 4.

The toroidal-field coils (TFCs) are copper-alloy bands positioned at the minor radius immediately outside the $\Delta b = 0.3$ -m-thick shield/test cell region. Although the TFCs operate at low fields, even during the startup phase when most of the plasma internal toroidal flux is provided from the PFC set through the RFP dynamo; magnetic ripple and magnetic islands, however, represent a major design constraint. The magnitude of the radial magnetic ripple relative to the poloidal field, $\Delta B_R/B_\theta$, is obtained from two-dimensional field-line tracings at the plasma (toroidal-field-reversal) surface. Generally, magnetic islands can be kept acceptably small relative to the distance between the toroidal-field reversal layer and the first wall if $\Delta B_R/B_\theta \leq 0.003$. Applying this constraint leads to the TFC design summarized in Table V and illustrated on Fig. 4.

The divertor-field (DF) coils represent the last major component of the FTF/RFP magnetics design and consist of a single nulling coil with flanking coils on each side to minimize the perturbation of the reversed toroidal field. Table V gives the main parameters for the DFs, with the results given in Ref. 11 indicating that four such divertor units, coupled to a highly radiating plasma ($f_{RAD} \geq 0.8$), would adequately control the heat and particle load envisaged for the $L_w = 5$ -MW/m² design (Table III).

4. SUMMARY AND CONCLUSIONS

Preliminary scoping studies⁹ of ignition/burn as well as fusion-test facilities (FTF) based on compact, high-power-density RFPs have been extended and continue a promising trend toward an economic commercial reactor. The degree of compactness that can be achieved for these pre-commercial devices, however, depends sensitively on the achievable beta and transport, as well as the need for effective current drive,¹⁴ control of eddy and image currents, and the careful management of particle and energy fluxes.¹¹ The next-step RFP devices⁹ (e.g., ZTH and RFX) will provide within the 1990-92 time frame the main physics database needed to achieve RFP ignition/burn, and ultimately the FTF/RFP steady-state parameters needed for eventual extension into an interesting

TABLE IV. PFC PARAMETERS FOR THE FTF/RFP

Parameter	Value	
	OHC	EFC
Current (MA)	15.02 ^(a) /(-26.53) ^(b)	11.51
Volume (m ³)	12.27	17.23
Mass (tonne)	90.32	126.80
Joule losses (MW)	29.94 ^(c) /93.43 ^(b)	55.14 ^(a)
Peak field (T)	7.93 ^(b)	4.06 ^(a)
Current density (MA/m ²)	12.3-23.2 ^(b)	30.6-32.8 ^(a)
EFC vertical field index	--	0.63
OHC stray vertical field (mT) ^(b)	1.22 (< 1.33)	--
PFC vertical transparency (%)	--	41.5

- (a) Steady-state values.
- (b) Back-bias values.
- (c) Forward-bias values.

TABLE V. TFC and DFC DESIGN PARAMETERS for the FTF/RFP

Parameter	Value		
	TFC	DFC	
		Nulling	Flanking
Number of TFCs	28	4	8
Major radius (m)	1.80	1.87	1.85
Minor radius (m)	0.67	0.54	0.53
Radial thickness (mm)	73.4	43.8	62.0
Toroidal thickness (mm)	245.6	43.8	32.0
Current per coil (kA)	168.3	384.7	192.2
Current density (MA/m ²)	9.3	200	50
Total ohmic power (MW)	5.3	30.0	7.2

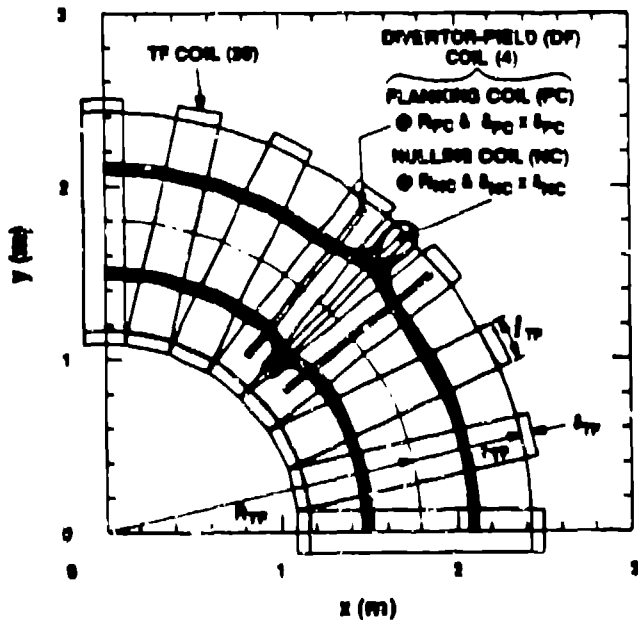


Fig. 4. Plan view of FTF/RFP torus showing (a) TFCs that meet the $\Delta B_R/B_0 \leq 0.003$ ripple constraint and (b) the poloidally symmetric toroidal-field divertor.

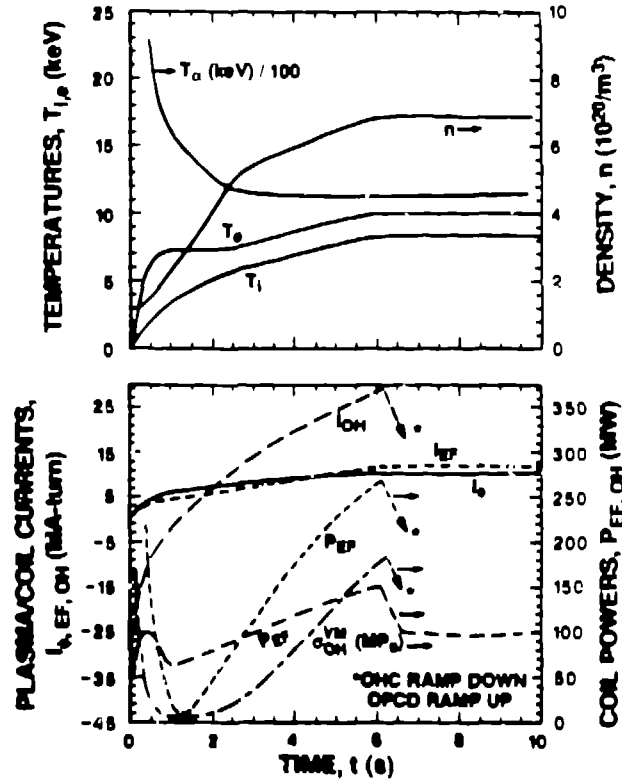


Fig. 5. Typical plasma and circuit responses for an ohmically-heated startup of the FTF/RFP device.

REFERENCES

1. K. Ogawa, et al., Proc. 9th Int. Conf. on Plasma Physics and Controlled Nuclear Fusion Research 1, 575-585, Baltimore, MD (September 1-8, 1982) IAEA Vienna
2. H. A. B. Bodin and G. Regstani, "The RFX Experiment Technical Proposal," Culham Laboratory report RFX-P1 (1981).
3. M. K. Buvir, et al., Paper D-II-3, Proc. 10th Int. Conf. on Plasma Physics and Controlled Nucl. Fusion, London, UK (September 12-19, 1984).
4. T. Tamano, et al., paper D-II-1, Proc. 10th Int. Conf. on Plasma Physics and Controlled Nucl. Fusion, London, UK (September 12-19, 1984).
5. D. A. Baker, et al., Proc. 10th Int. Conf. on Plasma Physics and Controlled Nuclear Fusion Research, London, UK (September 12-19, 1984).
6. D.B. Thornson (ed.), Proc. Int. Workshop on Engineering Design of Next Step Reversed Field Pinch Devices, Los Alamos National Laboratory (July 13-17, 1987).
7. C. Caperhaver, et al., "Compact Reversed-Field Pinch Reactors (CRFPR): Fusion-Power-Core Integration Study," Los Alamos National Laboratory report LA-10500-MS (1985).
8. The TITAN Research Group, "The TITAN Reversed-Field Pinch Reactor Study-The Final Report," University of California-Los Angeles, GA Technologies, Inc., Los Alamos National Laboratory, and Rensselaer Polytechnic Institute UCLA-PPG-1200 (to be published 1988).
9. C. G. Bethke, et al., Proc. 11th IEEE Symposium on Fusion Engineering, Austin, TX, p. 383 (November 18-22, 1985).
10. C. G. Bethke, et al., 13th Symposium on Fusion Tech. (SOFT), Varese, Italy (September 24-28, 1984).
11. K. A. Werley, et al., Proc. these proceedings.
12. P. Cooke, Proc. these proceedings.
13. R. L. Hagenson, et al., "Compact Reversed-Field Pinch Reactors (CRFPR): Preliminary Engineering Considerations," Los Alamos National Laboratory report LA-10200-MS (1984).
14. C. G. Bethke, "The Oscillating-Field Current Drive System," Proc. these proceedings.